

METHODOLOGY

Open Access



# Plasma microRNA biomarker detection for mild cognitive impairment using differential correlation analysis

Mitsunori Kayano<sup>1,2\*</sup> , Sayuri Higaki<sup>2</sup>, Jun-ichi Satoh<sup>3</sup>, Kenji Matsumoto<sup>4</sup>, Etsuro Matsubara<sup>5,6</sup>, Osamu Takikawa<sup>7</sup> and Shumpei Niida<sup>2</sup>

## Abstract

**Background:** Mild cognitive impairment (MCI) is an intermediate state between normal aging and dementia including Alzheimer's disease. Early detection of dementia, and MCI, is a crucial issue in terms of secondary prevention. Blood biomarker detection is a possible way for early detection of MCI. Although disease biomarkers are detected by, in general, using single molecular analysis such as t-test, another possible approach is based on interaction between molecules.

**Results:** Differential correlation analysis, which detects difference on correlation of two variables in case/control study, was carried out to plasma microRNA (miRNA) expression profiles of 30 age- and race-matched controls and 23 Japanese MCI patients. The 20 pairs of miRNAs, which consist of 20 miRNAs, were selected as MCI markers. Two pairs of miRNAs (hsa-miR-191 and hsa-miR-101, and hsa-miR-103 and hsa-miR-222) out of 20 attained the highest area under the curve (AUC) value of 0.962 for MCI detection. Other two miRNA pairs that include hsa-miR-191 and hsa-miR-125b also attained high AUC value of  $\geq 0.95$ . Pathway analysis was performed to the MCI markers for further understanding of biological implications. As a result, collapsed correlation on hsa-miR-191 and emerged correlation on hsa-miR-125b might have key role in MCI and dementia progression.

**Conclusion:** Differential correlation analysis, a bioinformatics tool to elucidate complicated and interdependent biological systems behind diseases, detects effective MCI markers that cannot be found by single molecule analysis such as t-test.

**Keywords:** Molecular network, Coexpression, Alzheimer's disease, Dementia

## Background

Early detection of dementia is a crucial issue in terms of secondary prevention. Mild cognitive impairment (MCI) is an intermediate state between normal aging and dementia including Alzheimer's disease [1–3]. On average, more than half MCI patients convert to dementia in 5 years, but some MCI patients remain stable or recover to normal over time [3–5]. This is why early detection and treatment of MCI is incredibly important.

Blood biomarkers can be useful for early detection of MCI. The present study is based on the hypothesis that neurite and synapse destruction, which are pathologic processes characteristic of early stages of AD, other neurodegenerative diseases, and MCI syndrome in general, can be detected in vitro by quantitative analysis of brain-enriched cell-free microRNA (miRNA) in the blood [6]. MiRNAs, a class of endogenous small non-coding RNAs, mediate posttranscriptional regulation of protein-coding genes by binding to the 3' untranslated region of target mRNAs, leading to translational inhibition or mRNA destabilization or degradation [7, 8]. Overall, the whole human miRNA regulates greater than 60% of all protein-coding genes [9]. Importantly, cell-free miRNA have been shown to be stable in blood samples [10], and aberrant

\*Correspondence: kayano@obihiro.ac.jp

<sup>1</sup>Research Center for Global Agromedicine, Obihiro University of Agriculture and Veterinary Medicine, Obihiro, Hokkaido, Japan

<sup>2</sup>Medical Genome Center, National Center for Geriatrics and Gerontology, Obu, Aichi, Japan

Full list of author information is available at the end of the article

**Table 1** Summary of participants in our study. Sample size, mean age and mean score of mini mental state exam (MMSE) are shown

Class		Total	Male	Female
Age-matched controls (Normal)	# of Participants	30	12	18
	Age	70.4	69.3	71.1
	MMSE	28.6	28.9	28.4
MCI patients	# of Participants	23	11	12
	Age	72.8	70.8	74.6
	MMSE	24.3	24.6	24.0

regulation of miRNA plays a central role in pathological events underlying cancers and neurodegenerative diseases [11–13].

A common statistical approach to detect disease biomarkers is differential expression analysis usually based on t-test between controls and patients [14]. Serum and plasma miRNA biomarkers for AD have been detected by differential expression analysis [15, 16]. Although differential expression analysis is a single molecular analysis, another possible approach is based on interaction between molecules. Such approaches, which are based on the interaction between molecules, can detect more stable and accurate biomarkers, since the interaction is array- and kit-free: a difference in mean can be easily affected by a small change in absolute expression value, but the interaction-based approach can be robust in that change. Differential correlation analysis (differential coexpression analysis, [17, 18]), an interaction-based approach, finds different types of biomarkers in terms of correlation change between controls and patients.

Differential correlation has been observed in AD and cancers [19, 20].

In this paper, differential correlation analysis was carried out to plasma miRNA expression profiles of 30 age-matched controls and 23 MCI patients in Japan. Pathway analysis was performed to the detected MCI biomarkers for further understanding of biological implications of the MCI markers.

**Methods**

**Participants**

The use of human volunteer in this study was approved by the Ethical Review Board of Japan’s National Center for Geriatrics and Gerontology (NCGG) and the Committee of Medical Ethics of Hirosaki University School of Medicine Institutional Review Board in Japan. We used blood samples collected in NCGG Biobank and Hirosaki University School of Medicine and Hospital. Written informed consent was obtained from all participants or their family prior to the study. The characteristics of the

**Table 2** 85 miRNAs in this study

hsa-let-7b	hsa-miR-142-5p	hsa-miR-186	hsa-miR-24	hsa-miR-374b
hsa-let-7d*	hsa-miR-143	hsa-miR-18a	hsa-miR-25	hsa-miR-378
hsa-let-7f	hsa-miR-144	hsa-miR-191	hsa-miR-26a	hsa-miR-423-3p
hsa-let-7g	hsa-miR-145	hsa-miR-192	hsa-miR-26b	hsa-miR-423-5p
hsa-let-7i	hsa-miR-146a	hsa-miR-197	hsa-miR-27a	hsa-miR-424
hsa-miR-101	hsa-miR-148a	hsa-miR-1979	hsa-miR-27b	hsa-miR-425
hsa-miR-103	hsa-miR-148b	hsa-miR-199a-3p	hsa-miR-29a	hsa-miR-425*
hsa-miR-106a	hsa-miR-150	hsa-miR-199a-5p	hsa-miR-29c	hsa-miR-451
hsa-miR-107	hsa-miR-151-3p	hsa-miR-19b	hsa-miR-30b	hsa-miR-484
hsa-miR-122	hsa-miR-151-5p	hsa-miR-20a	hsa-miR-30c	hsa-miR-486-5p
hsa-miR-125b	hsa-miR-152	hsa-miR-21	hsa-miR-30e	hsa-miR-505
hsa-miR-126	hsa-miR-15a	hsa-miR-22	hsa-miR-320a	hsa-miR-590-5p
hsa-miR-126*	hsa-miR-15b	hsa-miR-221	hsa-miR-320b	hsa-miR-652
hsa-miR-139-5p	hsa-miR-16	hsa-miR-222	hsa-miR-324-3p	hsa-miR-92a
hsa-miR-140-3p	hsa-miR-17	hsa-miR-223	hsa-miR-335	hsa-miR-93
hsa-miR-140-5p	hsa-miR-181a	hsa-miR-23a	hsa-miR-338-3p	hsa-miR-99a
hsa-miR-142-3p	hsa-miR-185	hsa-miR-23b	hsa-miR-342-3p	hsa-miR-99b

participants are shown in Table 1: the participants were 30 age- and race-matched controls (Normal, 12 males and 18 females, mean age of 70.4) and 23 Japanese MCI patients (11 males and 12 females, mean age of 72.8). In NCGG, amnesic MCI (MCI) was diagnosed following the criteria defined by Petersen et al. [5].

**Sample preparation**

Total RNA was extracted from plasma using the miRNeasy Mini Kit (Qiagen) according to the manufacturer’s instructions with the following modifications. Plasma was thawed on ice and centrifuged at 3000×g for 5 min in a 4 °C microcentrifuge. An aliquot of 200 μL of plasma per sample was transferred to a new tube and 750 μL of Qiazol mixture containing 1.25 μg/mL of MS2 bacteriophage RNA (Roche Applied Science) was added to the plasma. The tube was mixed and incubated for 5 min followed by the addition of 200 μL chloroform. The tube was mixed, incubated for 2 min and centrifuged at 12,000×g for 15 min in a 4 °C microcentrifuge. The upper aqueous phase was transferred to a new microcentrifuge tube and 1.5 volume of 100% ethanol was added. The contents were mixed thoroughly and 750 μL of the

sample was transferred to a Qiagen RNeasy Mini spin column in a collection tube followed by centrifugation at 15,000×g for 30 sec at room temperature. The process was repeated until all remaining sample had been loaded. The spin column was rinsed with 700 μL Qiagen RWT buffer and centrifuged at 15,000×g for 1 min at room temperature followed by another rinse with 500 μL Qiagen RPE buffer and centrifuged at 15,000×g for 1 min at room temperature. A rinse step (500 μL Qiagen RPE buffer) was repeated twice. The spin column was transferred to a new collection tube and centrifuged at 15,000×g for 2 min at room temperature. The spin column was transferred to a new microcentrifuge tube and the lid was left open for 1 min to allow the column to dry. Total RNA was eluted by adding 50 μL of RNase-free water to the membrane of the spin column and incubating for 1 min before centrifugation at 15,000×g for 1 min at room temperature. The RNA was stored in a –80 °C freezer.

**microRNA real-time qPCR**

For reverse transcription, 19.2 μL of RNA eluate was used in total 80 μL reactions with the miRCURY LNA™ Universal RT cDNA synthesis kit (Exiqon). The

**Table 3** Summary of the 20 pairs of miRNAs detected by differential correlation between Normal and MCI. The miRNA pairs are ranked by the difference of the correlation coefficients. The mean AUC value for the 20 miRNA pairs is 0.800 ± 0.051

Rank	Pair of miRNAs		r <sub>1</sub> - r <sub>2</sub>	log <sub>10</sub> p-value	AUC	Correlation Normal (r <sub>1</sub> )	Coefficients MCI (r <sub>2</sub> )
1	<b>hsa-miR-191</b>	<b>hsa-miR-590-5p</b>	0.963	-3.76	0.880	0.764	-0.200
2	<b>hsa-miR-125b</b>	<b>hsa-miR-18a</b>	0.930	-3.55	0.733	-0.218	0.712
3	<b>hsa-miR-140-3p</b>	hsa-miR-191	0.921	-2.85	0.800	0.540	-0.381
4	hsa-miR-103	hsa-miR-19b	0.917	-3.56	0.797	0.776	-0.141
5	hsa-miR-192	hsa-miR-197	0.912	-3.61	0.867	-0.281	0.631
6	<b>hsa-miR-191</b>	hsa-miR-19b	0.911	-4.10	0.854	0.826	-0.085
7	hsa-miR-152	<b>hsa-miR-191</b>	0.892	-3.42	0.863	0.772	-0.121
8	hsa-miR-103	<b>hsa-miR-590-5p</b>	0.888	-3.24	0.749	0.614	-0.275
9	<b>hsa-miR-191</b>	hsa-miR-320a	0.873	-3.38	0.872	0.691	-0.182
10	<b>hsa-miR-125b</b>	hsa-miR-20a	0.871	-3.80	0.801	-0.090	0.781
11	hsa-miR-106a	<b>hsa-miR-125b</b>	0.869	-3.94	0.785	-0.083	0.786
12	hsa-miR-101	hsa-miR-103	0.865	-3.65	0.768	0.805	-0.060
13	<b>hsa-miR-125b</b>	hsa-miR-24	0.840	-3.42	0.801	-0.073	0.768
14	hsa-miR-101	<b>hsa-miR-191</b>	0.831	-3.96	0.871	0.822	-0.009
15	hsa-miR-103	hsa-miR-222	0.828	-3.24	0.745	0.622	-0.207
16	hsa-miR-197	hsa-miR-378	0.820	-2.78	0.810	-0.234	0.586
17	hsa-miR-103	hsa-miR-223	0.815	-3.79	0.786	0.840	0.025
18	<b>hsa-miR-125b</b>	hsa-miR-223	0.815	-3.49	0.765	-0.015	0.800
19	hsa-let-7b	<b>hsa-miR-125b</b>	0.811	-3.75	0.718	-0.056	0.755
20	<b>hsa-miR-125b</b>	hsa-miR-484	0.801	-3.52	0.739	-0.078	0.723

Bold: top five miRNAs

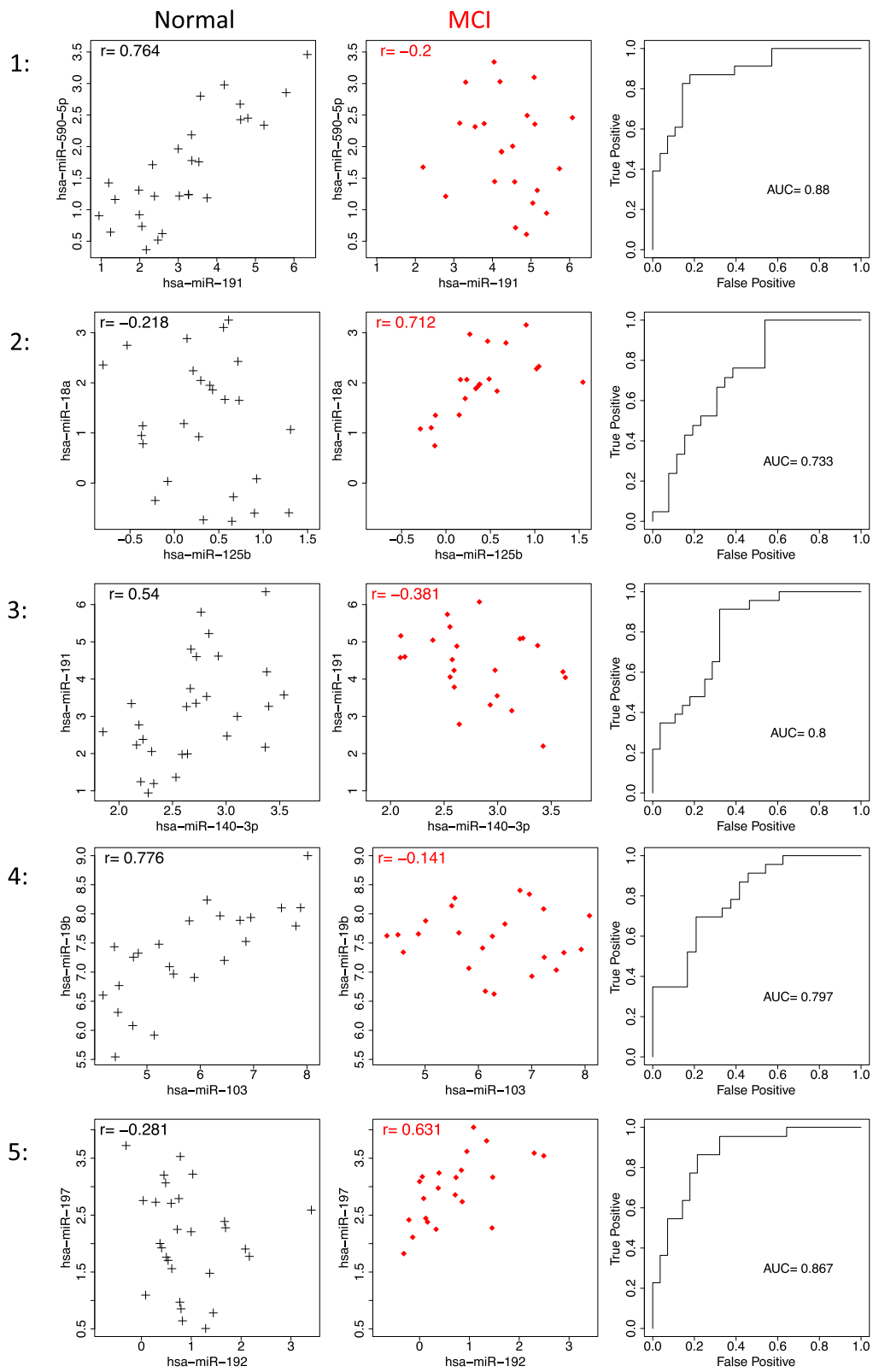


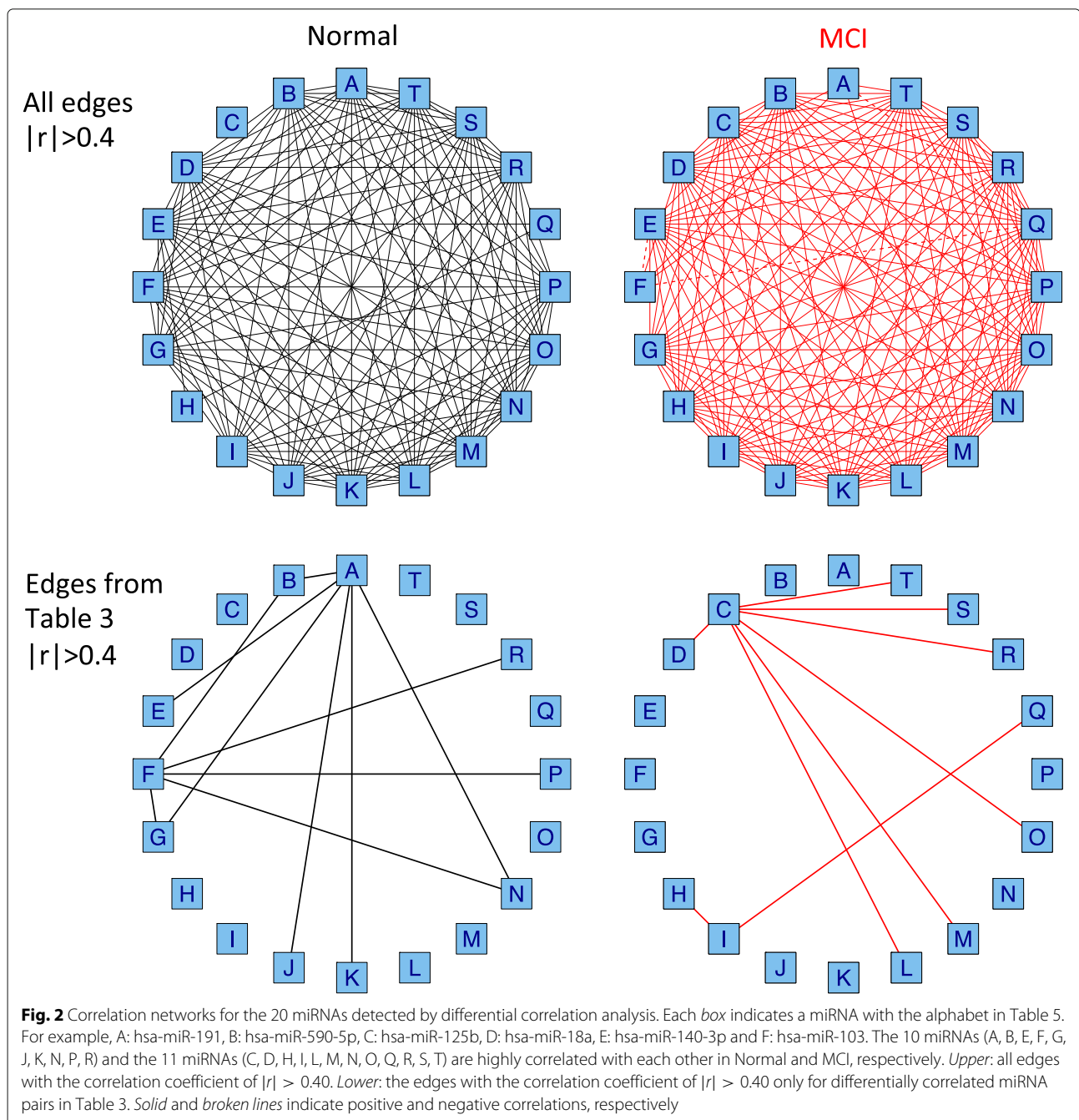
**Fig. 1** Scatterplots and ROC curves for top five miRNA pairs selected by differential correlation analysis. *Left:* Normal, *Middle:* MCI, *Right:* ROC curve

cDNA products were diluted 57.25 fold (80  $\mu$ L cDNA reactions + 4500  $\mu$ L water) and assayed in 10  $\mu$ L PCR reactions according to the protocol for the miR-CURY LNA™ Universal RT microRNA PCR System; each microRNA was assayed once by qPCR on the microRNA Ready-to-Use PCR, Human panel I and panel II, V2. Negative controls excluding template from the reverse transcription reaction were assayed and profiled in the same manner of the other samples. The amplification was performed in a LightCycler®480 Real-Time PCR System

(Roche) in 384 well plates. The amplification curves were analyzed using the Roche LC software (ver. 1.5), both for determination of Cp (by the second derivative method) and for melting curve analysis.

**Data filtering**

The raw data was extracted from the Light cycler 480 software. The GenEx software (Exiqon) was used for data filtering analysis. Any assay data value must be detected below Cp <37 or at least 3 Cp lower than negative



control value to be included in the data analysis. Data that did not pass these criteria were omitted from any further analysis. The amplification efficiency was calculated using the LinRegPCR software. Reactions with amplification efficiency below 1.6 were also removed. All data was normalized to the average of assays detected in each sample (-dCp= average Cp [ $<37$ ] - assay Cp). We then adopted 85 miRNAs out of 745 (Table 2) detected in over 80% samples in either one of the compared two conditions followed by filtering out low expression values ( $<20\%$ ).

**Differential correlation analysis**

Effective MCI markers can be found by differential correlation analysis, which investigates the difference of correlation coefficients between two classes of controls and MCI patients. In differential correlation analysis in our study, all possible miRNA pairs are ranked by the difference of two correlation coefficients

$$|r_1 - r_2|, \tag{1}$$

where  $r_1, r_2$  are Spearman's rank correlations of a miRNA pair for controls and MCI patients, respectively. MiRNA

pairs with a high score of (1) are candidates of MCI markers.

Differential correlation analysis in our study also provides the  $p$ -value of a pair of miRNAs as a reference for statistical significance of the difference of correlation coefficients. For this purpose, normalized rank correlation [21, 22],  $r_n$ , is utilized as a robust and Pearson-type correlation coefficient:

$$r_n = \frac{\sum_i \Phi^{-1}\{R_i/(n+1)\} \Phi^{-1}\{Q_i/(n+1)\}}{\sum_i [\Phi^{-1}\{i/(n+1)\}]^2}, \tag{2}$$

where  $\Phi$  is the distribution function of the standard normal distribution and  $R_i$  and  $Q_i$  are the ranks of the expression values  $x_i$  and  $y_i$  of two miRNAs, respectively. In our study, the value of normalized rank correlation  $r_n$  is quite similar with that of Spearman rank correlation: the mean of the difference between normalized rank correlations and Spearman's rank correlations for all miRNA pairs was only 0.001 in our data set. Hypothesis testing to investigate the equality of two normalized rank correlation coefficients is then applied according to a likelihood ratio test in [23, 24]. The  $p$ -value can be calculated through the hypothesis testing. We used Spearman's rank correlation for the difference calculation on correlation

**Table 4** Summary of the top 10 two-pairs of miRNAs out of the 20 miRNA pairs detected by differential correlation analysis in Table 3. The two-pairs of miRNAs are ranked by AUC value

Rank	AUC	Original Rank*	Original AUC*	Two-pairs of miRNAs		Correlation Normal ( $r_1$ )	Coefficients MCI ( $r_2$ )
1	0.962	14	0.871	hsa-miR-101	<b>hsa-miR-191</b>	0.822	-0.009
		15	0.745	hsa-miR-103	hsa-miR-222	0.622	-0.207
2	0.959	5	0.867	hsa-miR-192	hsa-miR-197	-0.281	0.631
		14	0.871	hsa-miR-101	<b>hsa-miR-191</b>	0.822	-0.009
3	0.958	6	0.854	<b>hsa-miR-191</b>	hsa-miR-19b	0.826	-0.085
		17	0.786	hsa-miR-103	hsa-miR-223	0.840	0.025
4	0.957	1	0.880	<b>hsa-miR-191</b>	<b>hsa-miR-590-5p</b>	0.764	-0.200
		17	0.786	hsa-miR-103	hsa-miR-223	0.840	0.025
5	0.957	14	0.871	hsa-miR-101	<b>hsa-miR-191</b>	0.822	-0.009
		16	0.810	hsa-miR-197	hsa-miR-378	-0.234	0.586
6	0.952	12	0.768	hsa-miR-101	hsa-miR-103	0.805	-0.060
		13	0.801	<b>hsa-miR-125b</b>	hsa-miR-24	-0.073	0.768
7	0.951	5	0.867	hsa-miR-192	hsa-miR-197	-0.281	0.631
		9	0.872	<b>hsa-miR-191</b>	hsa-miR-320a	0.691	-0.182
8	0.951	14	0.871	hsa-miR-101	<b>hsa-miR-191</b>	0.822	-0.009
		17	0.786	hsa-miR-103	hsa-miR-223	0.840	0.025
9	0.951	1	0.880	<b>hsa-miR-191</b>	<b>hsa-miR-590-5p</b>	0.764	-0.200
		15	0.745	hsa-miR-103	hsa-miR-222	0.622	-0.207
10	0.947	4	0.797	hsa-miR-103	hsa-miR-19b	0.776	-0.141
		14	0.871	hsa-miR-101	<b>hsa-miR-191</b>	0.822	-0.009

\*: Original rank and AUC of each pair of miRNAs in Table 3. Bold: top five miRNAs

coefficients (1) and used the normalized rank correlation for  $p$ -value calculation.

Evaluation of the performance of a miRNA pair as MCI marker is not straight-forward. We here apply receiver-operator characteristic (ROC) analysis on logistic regression with an interaction term of two miRNAs:

$$\log \frac{p}{1-p} = \beta_0 + \beta_1 X_1 + \beta_2 X_2 + \beta_{12} X_1 X_2 \quad (3)$$

where  $p$  is the probability that a sample is in MCI class,  $\beta_0, \beta_1, \beta_2, \beta_{12}$  are regression coefficients and  $X_1, X_2$  are the expression value of two miRNAs, respectively. The interaction term  $\beta_{12} X_1 X_2$  is essential for the evaluation of two miRNAs detected by differential correlation analysis. If the correlation coefficient between  $X_1$  and  $X_2$  is altered between controls and MCI class, then the interaction term significantly affects the discrimination of MCI from controls. The area under the curve (AUC) value (=0 to 1) is estimated through ROC analysis based on the estimated probabilities  $\hat{p}_1, \dots, \hat{p}_n$  for all samples of controls and MCI patients. If the estimated probabilities for controls and MCI patients are much different (e.g.,  $\hat{p} < 0.5$  for controls and  $\hat{p} > 0.5$  for MCI patients), then AUC value will be 1 (completely separated). In order to evaluate of the performance of several pairs of miRNAs as MCI markers, logistic regression with multiple interaction terms can be available:

$$\log \frac{p}{1-p} = \beta_0 + \beta_1 X_1 + \beta_2 X_2 + \dots + \beta_k X_k + \sum_{(i,j) \in C} \beta_{ij} X_i X_j \quad (4)$$

where  $C$  is a set of miRNA pairs that are differentially correlated between controls and MCI patients. For example, four miRNA pairs (miRNA 1-2, 1-3, 3-4 and 4-5) with five miRNAs can be incorporated in the logistic regression model,  $\log p/(1-p) = \beta_0 + \beta_1 X_1 + \beta_2 X_2 + \beta_3 X_3 + \beta_4 X_4 + \beta_5 X_5 + \beta_{12} X_1 X_2 + \beta_{13} X_1 X_3 + \beta_{34} X_3 X_4 + \beta_{45} X_4 X_5$ , where  $C = \{(1, 2), (1, 3), (3, 4), (4, 5)\}$  in the interaction terms  $\sum_{(i,j) \in C} \beta_{ij} X_i X_j$ . ROC analysis evaluates the performance of the five miRNAs as MCI markers simultaneously.

## Results

### Differential correlation analysis

Differential correlation analysis was applied to the data set with 85 miRNAs for age-matched samples of 30 controls and 23 MCI patients (Tables 1 and 2). The 3570 possible pairs from the 85 miRNAs were ranked, according to the difference of correlation coefficients between controls and MCI patients. The 20 pairs of miRNAs, which had the difference of correlation coefficients of  $|r_1 - r_2| > 0.8$ , were selected as biomarkers that distinguish MCI patients

from controls (Table 3). The AUC value by each of the 20 miRNA pairs was  $0.800 \pm 0.051$  ranged between 0.718 and 0.880. Figure 1 shows scatterplots and ROC curves for each of top five miRNA pairs selected by differential correlation between normal and MCI (see also Additional file 1 for the remained miRNA pairs). Figure 2 shows correlation networks of the 20 miRNA pairs.

AUC value for all two-pairs of the 20 miRNA pairs was also calculated by using (4). Table 4 shows summary of the top 10 two-pairs of miRNAs out of 190 possible pairs. Two miRNA pairs (hsa-miR-191 and hsa-miR-101, and hsa-miR-103 and hsa-miR-222) attained the highest AUC value of 0.962 for MCI detection (Fig. 3). Other two miRNA pairs that include hsa-miR-191 and hsa-miR-125b also attained high AUC value of  $\geq 0.95$  (Table 4).

### Pathway analysis

We performed Ingenuity Pathway Analysis (IPA) about correlation networks to be lost and emerged in the MCI. Figures 4 and 5 show estimated networks through IPA on the 10 and 11 miRNAs, which are highly correlated with each other in Normal and MCI respectively. IPA revealed that the 10 highly correlated miRNAs in Normal were composed of networks surrounding Akt, IGF1, PPARA, IL6 and AGO2 genes. The IPA showed that TP53 genes directly regulated all of 11 highly correlated miRNAs in MCI. Pathways enriched for target genes of 10/11 highly

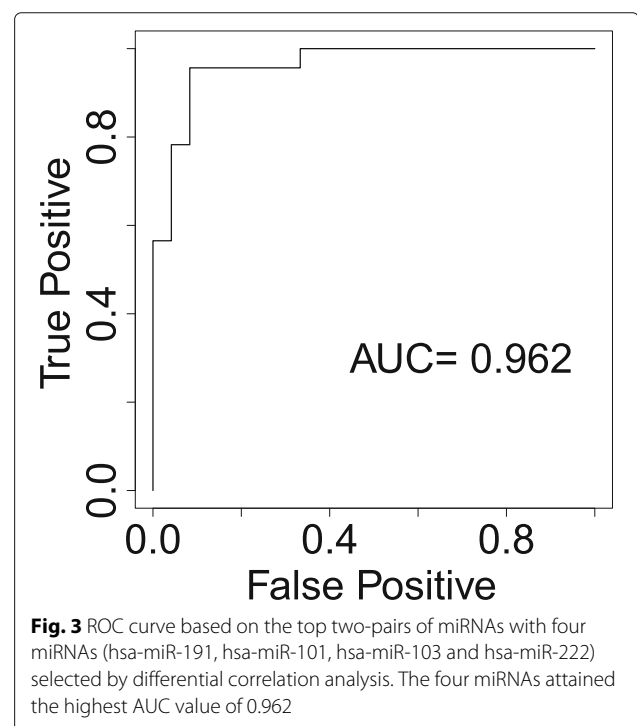
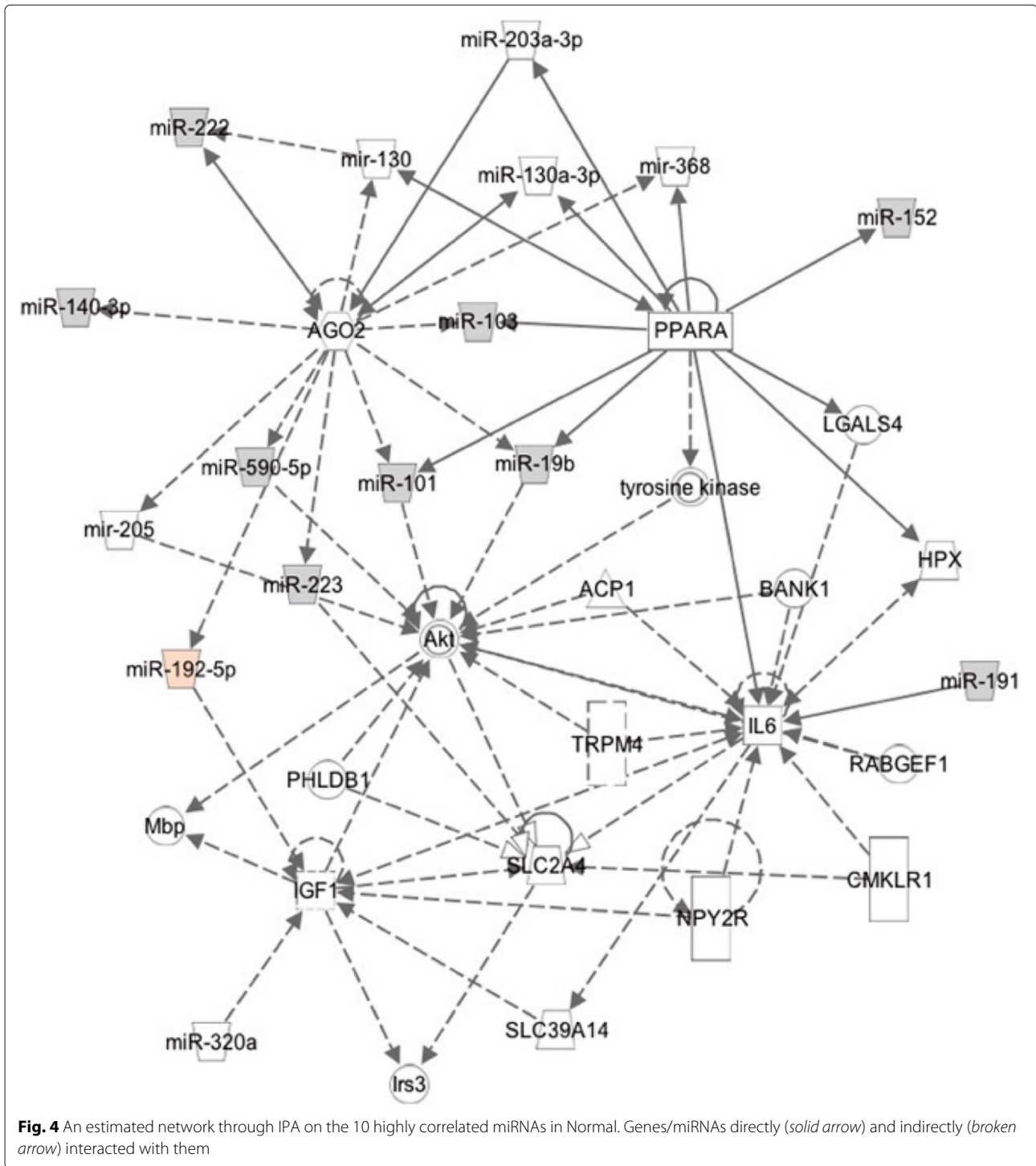


**Fig. 3** ROC curve based on the top two-pairs of miRNAs with four miRNAs (hsa-miR-191, hsa-miR-101, hsa-miR-103 and hsa-miR-222) selected by differential correlation analysis. The four miRNAs attained the highest AUC value of 0.962



correlated miRNAs in Normal/MCI are shown in Tables 6 and 7.

**T-test**

Traditional t-test was applied to the same data set with 85 miRNAs for age-matched samples of 30 controls and 23

MCI patients (Tables 1 and 2). The detail was described in Additional file 2. The 22 miRNAs out of 85 were detected as MCI markers (Table 5 and Additional file 2). The AUC value by each of the 22 miRNAs was  $0.784 \pm 0.017$  ranged between 0.748 and 0.828. Importantly, differential correlation analysis detected much different and

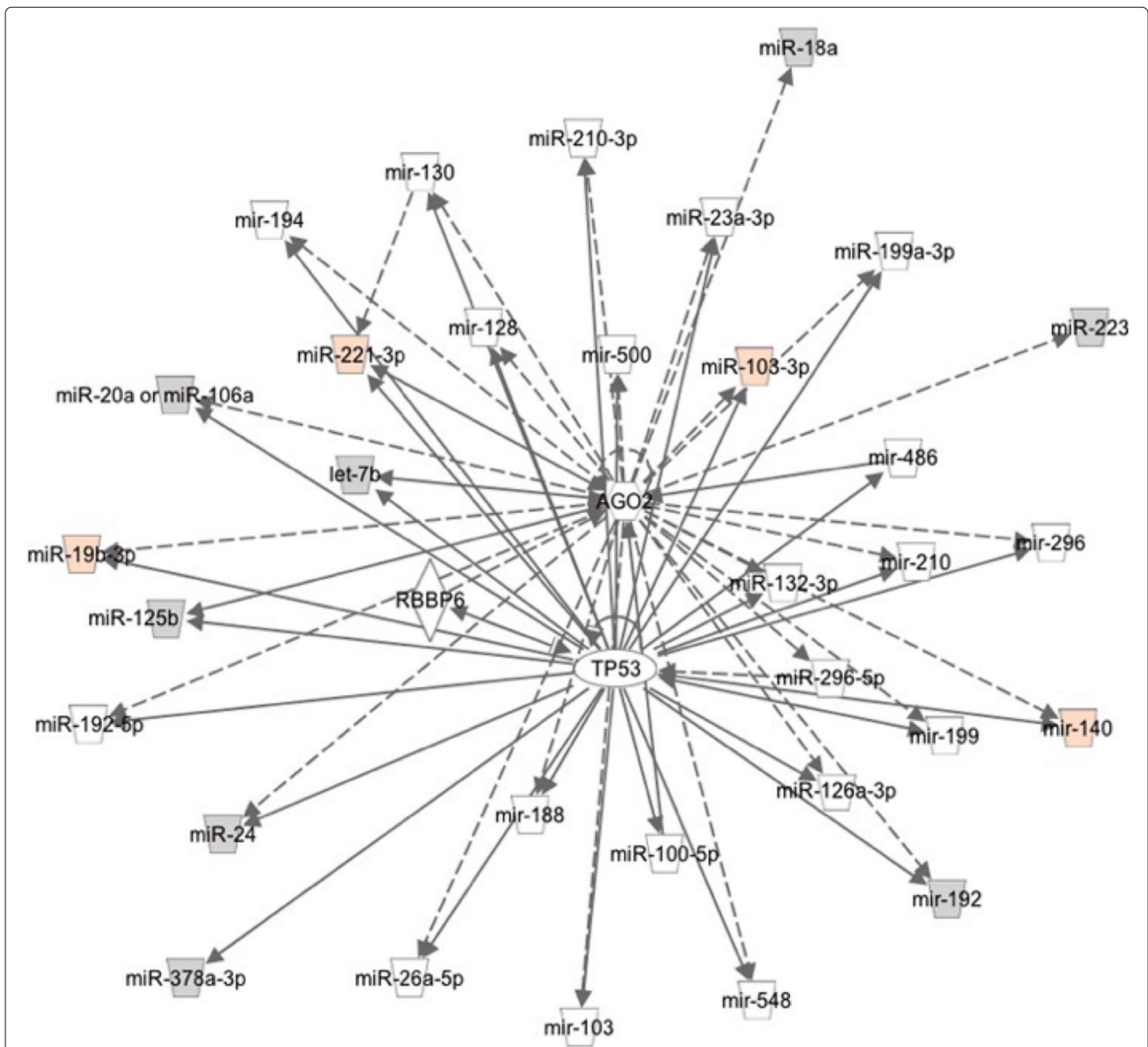


**Fig. 5** An estimated network through IPA on the 11 highly correlated miRNAs in MCI. Genes/miRNAs directly (solid arrow) and indirectly (broken arrow) interacted with them

more sensitive MCI markers compared to t-test (Table 5): mean AUC value =  $0.800 \pm 0.051$  (differential correlation analysis), =  $0.784 \pm 0.017$  (t-test). Also, the highest AUC value of any four miRNAs from the 22 miRNAs (Figure 4 in Additional file 2) was less than the highest in the two-pair approach, which investigate the performance of three to four miRNAs simultaneously, in differential correlation analysis.

**Discussion**

Pathway analysis, IPA, allows us for further understanding of biological implications of the detected 20 MCI

maker pairs of miRNA. Validation study and brain-based previous studies can support the results of differential correlation analysis and IPA.

IPA showed that 10 highly correlated miRNAs in Normal were composed of networks surrounding Akt, IGF1, PPARA, IL6 and AGO2 genes (Fig. 4). Akt, IGF1 and Irs3 are key molecules in insulin signaling pathway and PPARA is a regulator of lipid metabolism. Moreover, insulin, mTOR and PI3K-Akt signaling pathway were ranked among top 5 analyzed by DIANA-miRPath, which predicted miRNA targets through DIANA-microT-CDS and combined their interactions into KEGG pathway

**Table 5** The two sets of miRNAs detected by Left: differential correlation analysis and Right: t-test

Differential correlation 20 miRNAs		t-test 22 miRNAs			
A:	<b>hsa-miR-191</b>	L:	hsa-miR-20a	<b>hsa-miR-151-3p</b>	hsa-miR-15b
B:	<b>hsa-miR-590-5p</b>	M:	hsa-miR-106a	<b>hsa-miR-126*</b>	hsa-let-7d*
C:	<b>hsa-miR-125b</b>	N:	hsa-miR-101	<b>hsa-miR-23a</b>	<u>hsa-miR-197</u>
D:	<b>hsa-miR-18a</b>	O:	<u>hsa-miR-24</u>	<b>hsa-miR-27b</b>	hsa-miR-30b
E:	<b>hsa-miR-140-3p</b>	P:	hsa-miR-222	<b>hsa-miR-146a</b>	hsa-miR-185
F:	hsa-miR-103	Q:	hsa-miR-378	hsa-miR-30c	<u>hsa-miR-191</u>
G:	hsa-miR-19b	R:	<u>hsa-miR-223</u>	hsa-miR-151-5p	hsa-miR-26b
H:	hsa-miR-192	S:	hsa-let-7b	hsa-miR-23b	<u>hsa-miR-223</u>
I:	<u>hsa-miR-197</u>	T:	hsa-miR-484	hsa-miR-92a	hsa-miR-26a
J:	hsa-miR-152			<u>hsa-miR-24</u>	hsa-miR-16
K:	hsa-miR-320a			hsa-miR-144	hsa-let-7f

Bold: top five miRNAs in each analysis  
 Underline: same miRNAs in left and right sides  
 The alphabets in the left side are utilized in Fig. 2

**Table 6** Pathways enriched for target genes of 10 highly correlated miRNAs in Normal

# KEGG pathway	p-value	#genes	#miRNAs
1 Pathways in cancer (hsa05200)	$2.13 \times 10^{-19}$	101	9
2 Prostate cancer (hsa05215)	$3.39 \times 10^{-17}$	35	9
3 PI3K-Akt signaling pathway (hsa04151)	$1.92 \times 10^{-15}$	94	9
4 mTOR signaling pathway (hsa04150)	$6.11 \times 10^{-14}$	27	9
5 Insulin signaling pathway (hsa04910)	$1.18 \times 10^{-13}$	46	8
6 Endometrial cancer (hsa05213)	$4.34 \times 10^{-13}$	22	9
7 Ubiquitin mediated proteolysis (hsa04120)	$6.03 \times 10^{-13}$	46	10
8 Focal adhesion (hsa04510)	$5.48 \times 10^{-12}$	60	9
9 Non-small cell lung cancer (hsa05223)	$5.16 \times 10^{-10}$	21	8
10 Hedgehog signaling pathway (hsa04340)	$6.68 \times 10^{-10}$	20	7

**Table 7** Pathways enriched for target genes of 11 highly correlated miRNAs in MCI

# KEGG pathway	p-value	#genes	#miRNAs
1 MAPK signaling pathway (hsa04010)	$1.81 \times 10^{-13}$	79	11
2 Endocytosis (hsa04144)	$5.43 \times 10^{-12}$	63	10
3 TGF-beta signaling pathway (hsa04350)	$5.43 \times 10^{-12}$	31	10
4 PI3K-Akt signaling pathway (hsa04151)	$3.88 \times 10^{-10}$	91	11
5 Pathways in cancer (hsa05200)	$4.62 \times 10^{-10}$	92	11
6 Neurotrophin signaling pathway (hsa04722)	$5.66 \times 10^{-8}$	38	11
7 Prostate cancer (hsa05215)	$6.03 \times 10^{-8}$	30	10
8 Ubiquitin mediated proteolysis (hsa04120)	$1.37 \times 10^{-7}$	41	11
9 ErbB signaling pathway (hsa04012)	$5.11 \times 10^{-7}$	29	10
10 Hepatitis B (hsa05161)	$6.96 \times 10^{-7}$	41	11

(Table 6). These pathways included target genes of 9 miRNAs except for miR-191. Previous studies consistently reported that identified biomarkers, changed genes and networks in AD patients or AD model were involved in insulin-related signaling [8, 25, 26]. Indeed, experimentally validated evidences support key role of miR-103a-3p, miR-320a and miR-590-5p in metabolic pathway [27, 28] and miR-103a-3p association with AD [29–31]. In Fig. 2, we found that miR-103a-3p and miR-191 served as hub miRNAs of 12 edges of pair correlations in Normal. miR-191 is also a widely used biomarker for diseases like cancers, type-2 diabetes and AD [32]. Considering the significant upregulation of miR-191 in MCI (t-test), these findings supposed that MCI stage lost miRNA correlations as cause and/or effect of changed expression balance among miR-191 and members in insulin related signaling. Lost of their correlation could become a discriminative marker for MCI.

There are newly emerged correlation network with a hub miRNA, miR-125b in MCI patient plasma. The IPA showed that TP53 genes directly regulated all of 11 highly correlated miRNAs in MCI (Fig. 5). TP53 has been explored originally as a tumor suppressor, but recently reported about other aspects to control diseases such as aging and metabolism [33]. There are accumulated studies that the change of TP53 protein, its modification and conformation were observed in AD patient brains [34–36] and blood [37]. Intriguingly, Le et al. demonstrated that miR-125b bound to 3' untranslated region of TP53 mRNA and worked as a negative regulator of TP53 [38], which means a possible presence of negative feedback loop. The result of DIANA-miRPath indicated that MAPK, TGF-beta and Neurotrophin signaling pathway were characteristic in MCI, although there were overlapped pathways in Normal and MCI (Table 7). Similarly to TP53 signaling, these pathways have common biological functions such as cell survival, cell cycle and apoptosis. In this study, change of TP53 function might be detected as generated new correlations of the downstream miRNAs.

This study focuses on biomarker detection for MCI, not on mechanism that how were plasma miRNAs produced from brain. However, brain-based studies also support reliability of hsa-miR-191 and hsa-125b as MCI markers. For example, expression change of miR-191 is required for maintenance of spine restructuring in mouse hippocampus [39], and miR-125b effects on dendritic spine morphology and synaptic physiology in hippocampal neurons of mouse [40], where it has been shown that MCI and AD is a synaptic failure [41–43].

In summary, collapsed correlation on hsa-miR-191 and emerged correlation on hsa-miR-125b might have key role in MCI, and dementia progression.

## Conclusions

Differential correlation analysis, which detects difference of correlation in case/control study, was carried out to plasma miRNA expression profiles of 30 age- and race-matched controls and 23 Japanese MCI patients. The 20 miRNA pairs were selected as biomarkers for MCI. The 20 miRNAs were more sensitive and different from that by t-test.

Pathway analysis showed that, in particular, collapsed correlation on hsa-miR-191 and emerged correlation on hsa-miR-125b might have key role in MCI, and dementia progression. Differential correlation analysis detects effective MCI markers that cannot be found by single molecule analysis such as t-test. Also, differential correlation analysis could be a key bioinformatics tool to find sensitive biomarkers and to elucidate complicated biological systems behind diseases.

## Additional files

**Additional file 1:** Supplement A. Scatterplots and ROC curves for each of top 20 pairs of miRNAs selected by differential correlation analysis between Normal and MCI. (PDF 63.2 kb)

**Additional file 2:** Supplement B. Details of t-test and the results. The results include boxplots and ROC curves based on each of 22 miRNAs selected by t-test between Normal and MCI. (PDF 55.1 kb)

## Abbreviations

AD: Alzheimer's disease; AUC: Area under the (ROC) curve; IPA: Ingenuity pathway analysis; MCI: Mild cognitive impairment; miRNA: MicroRNA; MMSE: Mini mental state exam; NCGG: National center for geriatrics and gerontology; ROC: Receiver-operator characteristic

## Acknowledgements

Not applicable.

## Funding

This work has been supported in part by the Program for Promotion of Fundamental Studies in Health Sciences conducted from the National Institute of Biomedical Innovation of Japan (10-43 and 10-44), the Research Funding for Longevity Sciences from National Center for Geriatrics and Gerontology, Japan (23-9 and 26-20), and KAKENHI #24700290 from Japan Society for the Promotion of Science.

## Availability of data and materials

Data will be available from NCGG Biobank (Medical Genome Center, <http://www.ncgg.go.jp/mgc/index.html> [In preparing to upload the data]). If you have any problems to access the web site, please contact author.

## Authors' contributions

MK, SH, KM, EM, OT and SN designed the study. MK, SH, KM and EM performed the analysis. MK and SH wrote the manuscript. JS, OT and SN contributed to critical review of the manuscript. All authors read and approved the final manuscript.

## Competing interests

The authors declare that they have no competing interests.

## Consent for publication

Not applicable.

## Ethics approval and consent to participate

The use of human volunteer in this study was approved by the Ethical Review Board of Japan's National Center for Geriatrics and Gerontology (NCGG) and the Committee of Medical Ethics of Hirosaki University School of Medicine

Institutional Review Board in Japan: reference number of 443-6 (Approved 26 February 2015), 2008-116 (Approved 28 November 2008). We used blood samples collected in NCGG Biobank and Hirosaki University School of Medicine and Hospital. Written informed consent was obtained from all participants or their family prior to the study.

#### Author details

<sup>1</sup>Research Center for Global Agromedicine, Obihiro University of Agriculture and Veterinary Medicine, Obihiro, Hokkaido, Japan. <sup>2</sup>Medical Genome Center, National Center for Geriatrics and Gerontology, Obu, Aichi, Japan. <sup>3</sup>Department of Bioinformatics and Molecular Neuropathology, Meiji Pharmaceutical University, Kiyose, Tokyo, Japan. <sup>4</sup>Department of Allergy and Clinical Immunology, National Center for Child Health and Development, Setagaya, Tokyo, Japan. <sup>5</sup>Department of Neurology, Hirosaki University Graduate School of Medicine, Hirosaki, Aomori, Japan. <sup>6</sup>Department of Neurology, Oita University Faculty of Medicine, Yufu, Oita, Japan. <sup>7</sup>Innovation Center for Clinical Research, National Center for Geriatrics and Gerontology, Obu, Aichi, Japan.

Received: 27 September 2016 Accepted: 22 November 2016

Published online: 12 December 2016

#### References

- DeCarli C. Mild cognitive impairment: prevalence, prognosis, aetiology, and treatment. *Lancet Neurol.* 2003;2(1):15–21.
- Markesbery WR. Neuropathologic alterations in mild cognitive impairment: a review. *J Alzheimers Dis: JAD.* 2010;19(1):221.
- Apostolova LG, Thompson PM, Green AE, Hwang KS, Zoumalan C, Jack CR, et al. 3D comparison of low, intermediate, and advanced hippocampal atrophy in MCI. *Hum Brain Mapp.* 2010;31(5):786–97.
- Gauthier S, Reisberg B, Zaudig M, Petersen RC, Ritchie K, Broich K, et al. Mild cognitive impairment. *Lancet.* 2006;367(9518):1262–70.
- Petersen RC, Doody R, Kurz A, Mohs RC, Morris JC, Rabins PV, et al. Current concepts in mild cognitive impairment. *Arch Neurol.* 2001;58(12):1985–92.
- Sheinerman KS, Tsvinsky VG, Crawford F, Mullan MJ, Abdullah L, Umansky SR. Plasma microRNA biomarkers for detection of mild cognitive impairment. *Aging (Albany NY).* 2012;4(9):590.
- Guo H, Ingolia NT, Weissman JS, Bartel DP. Mammalian microRNAs predominantly act to decrease target mRNA levels. *Nature.* 2010;466(7308):835–40.
- Satoh Ji, Kino Y, Niida S. MicroRNA-Seq Data Analysis Pipeline to Identify Blood Biomarkers for Alzheimer's Disease from Public Data. *Biomark Insights.* 2015;10:21.
- Friedman RC, Farh KKH, Burge CB, Bartel DP. Most mammalian mRNAs are conserved targets of microRNAs. *Genome Res.* 2009;19(1):92–105.
- Mitchell PS, Parkin RK, Kroh EM, Fritz BR, Wyman SK, Pogosova-Agadjanyan EL, et al. Circulating microRNAs as stable blood-based markers for cancer detection. *Proc Natl Acad Sci.* 2008;105(30):10513–8.
- Keller A, Leidinger P, Bauer A, ElSharawy A, Haas J, Backes C, et al. Toward the blood-borne miRNome of human diseases. *Nat Methods.* 2011;8(10):841–3.
- Satoh Ji. Molecular network analysis of human microRNA targetome: from cancers to Alzheimer's disease. *BioData Min.* 2012;5(1):17.
- Hayes J, Peruzzi PP, Lawler S. MicroRNAs in cancer: biomarkers, functions and therapy. *Trends Mol Med.* 2014;20(8):460–9.
- Cui X, Churchill GA, et al. Statistical tests for differential expression in cDNA microarray experiments. *Genome Biol.* 2003;4(4):210.
- Kumar P, Dezzo Z, Mackenzie C, Oestreicher J, Agoulnik S, Byrne M, et al. Circulating miRNA biomarkers for Alzheimer's disease. *PLoS one.* 2013;8(7):e69807.
- Tan L, Yu JT, Liu QY, Tan MS, Zhang W, Hu N, et al. Circulating miR-125b as a biomarker of Alzheimer's disease. *J Neurol Sci.* 2014;336(1):52–6.
- de la Fuente A. From 'differential expression' to 'differential networking'—identification of dysfunctional regulatory networks in diseases. *Trends Genet.* 2010;26(7):326–33.
- Kayano M, Shiga M, Mamitsuka H. Detecting differentially coexpressed genes from labeled expression data: a brief review. *Comput Biol Bioinforma IEEE/ACM Trans.* 2014;11(1):154–67.
- Choi Y, Kendziorski C. Statistical methods for gene set co-expression analysis. *Bioinformatics.* 2009;25(21):2780–6.
- Amar D, Safer H, Shamir R. Dissection of regulatory networks that are altered in disease via differential co-expression. *PLoS Comput Biol.* 2013;9(3):e1002955.
- Yanagawa T, Kobayashi Y, Nagayama J. Assessing the joint effects of chlorinated dioxins, some pesticides and polychlorinated biphenyls on thyroid hormone status in Japanese breast-fed infants. *Environmetrics.* 2003;14(2):121–8.
- Kayano M, Imoto S, Yamaguchi R, Miyano S. Multi-omics Approach for Estimating Metabolic Networks Using Low-Order Partial Correlations. *J Comput Biol.* 2013;20(8):571–82.
- Paul S. Test for the equality of several correlation coefficients. *Can J Stat.* 1989;17:27.
- Kayano M, Takigawa I, Shiga M, Tsuda K, Mamitsuka H. ROS-DET: robust detector of switching mechanisms in gene expression. *Nucleic Acids Res.* 2011;39(11):e74–e74.
- Liang D, Han G, Feng X, Sun J, Duan Y, Lei H. Concerted perturbation observed in a hub network in Alzheimer's disease. *PLoS One.* 2012;7(7):e40498.
- Jackson HM, Soto I, Graham LC, Carter GW, Howell GR. Clustering of transcriptional profiles identifies changes to insulin signaling as an early event in a mouse model of Alzheimer's disease. *BMC Genomics.* 2013;14(1):831.
- Karolina DS, Tavintharan S, Armugam A, Sepramaniam S, Pek SLT, Wong MT, et al. Circulating miRNA profiles in patients with metabolic syndrome. *J Clin Endocrinol Metab.* 2012;97(12):E2271–E6.
- Williams MD, Mitchell GM. MicroRNAs in insulin resistance and obesity. *Exp Diabetes Res.* 2012;484696.
- Wang WX, Rajeev BW, Stromberg AJ, Ren N, Tang G, Huang Q, et al. The expression of microRNA miR-107 decreases early in Alzheimer's disease and may accelerate disease progression through regulation of  $\beta$ -site amyloid precursor protein-cleaving enzyme 1. *J Neurosci.* 2008;28(5):1213–23.
- Yao J, Hennessey T, Flynt A, Lai E, Beal MF, Lin MT. MicroRNA-related cofilin abnormality in Alzheimer's disease. *PLoS One.* 2010;5(12):e15546.
- Moncini S, Salvi A, Zuccotti P, Viero G, Quattrone A, Barlati S, et al. The role of miR-103 and miR-107 in regulation of CDK5R1 expression and in cellular migration. *PLoS One.* 2011;6(5):e20038.
- Nagpal N, Kulshreshtha R. miR-191: an emerging player in disease biology. *Front Genet.* 2014;5:99.
- Vousden KH, Lane DP. p53 in health and disease. *Nature Reviews Molecular Cell Biology.* 2007;8(4):275–283.
- Kitamura Y, Shimohama S, Kamoshima W, Matsuoka Y, Nomura Y, Taniguchi T. Changes of p53 in the brains of patients with Alzheimer's disease. *Biochem Biophys Res Commun.* 1997;232(2):418–21.
- Di Domenico F, Cenini G, Sultana R, Perluigi M, Uberti D, Memo M, et al. Glutathionylation of the pro-apoptotic protein p53 in Alzheimer's disease brain: implications for AD pathogenesis. *Neurochem Res.* 2009;34(4):727–33.
- Stanga S, Lanni C, Govoni S, Uberti D, D'Orazi G, Racchi M. Unfolded p53 in the pathogenesis of Alzheimer's disease: is HIPK2 the link. *Aging (Albany NY).* 2010;2(9):545.
- Uberti D, Lanni C, Racchi M, Govoni S, Memo M. Conformationally altered p53: a putative peripheral marker for Alzheimer's disease. *Neurodegener Dis.* 2008;5(3-4):209–11.
- Le MT, Teh C, Shyh-Chang N, Xie H, Zhou B, Korzh V, et al. MicroRNA-125b is a novel negative regulator of p53. *Gene Dev.* 2009;23(7):862–76.
- Hu Z, Yu D, Gu Qh, Yang Y, Tu K, Zhu J, et al. miR-191 and miR-135 are required for long-lasting spine remodelling associated with synaptic long-term depression. *Nat Commun.* 2014;5:3263.
- Edbauer D, Neilson JR, Foster KA, Wang CF, Seeburg DP, Batterton MN, et al. Regulation of synaptic structure and function by FMRP-associated microRNAs miR-125b and miR-132. *Neuron.* 2010;65(3):373–84.
- Terry RD, Masliah E, Salmon DP, Butters N, DeTeresa R, Hill R, et al. Physical basis of cognitive alterations in Alzheimer's disease: synapse loss is the major correlate of cognitive impairment. *Ann Neurol.* 1991;30(4):572–80.
- Selkoe DJ. Alzheimer's disease is a synaptic failure. *Science.* 2002;298(5594):789–91.
- Scheff SW, Price DA, Schmitt FA, Mufson EJ. Hippocampal synaptic loss in early Alzheimer's disease and mild cognitive impairment. *Neurobiol Aging.* 2006;27(10):1372–84.